



OPEN

Modeling the impact of extreme weather events and future climate on the radiologically contaminated sites of Enewetak Atoll

Lakshitha Premathilake[✉], Saikat Ghosh, Rajiv Prasad, Sourav Taraphdar, Taiping Wang, Tarang Khangaonkar, Bruce Napier, Tracy Ikenberry & Lai-yung Leung

Enewetak Atoll underwent 43 historical nuclear tests from 1948 to 1958, including the first hydrogen bomb test, resulting in a substantial nuclear material fallout contaminating the Atoll and the lagoon waters. The radionuclide fallout material deposited in lagoon sediments and soil on the islands will remain for decades to come. With intensifying climate and extreme weather events, the possibility of redistribution of deposited radionuclide material has become a great concern. This study uses a numerical modeling approach to estimate the potential elevated radionuclide concentrations that can be distributed during storm events under current and future climates. We simulated three historical storm scenarios that are most likely to impact Atoll's environment and remobilize the radionuclide-bound sediments. WRF-ARW was used to reconstruct these storm scenarios under current year (2015) and future year (2090) climates. Storm-induced ocean hydrodynamics conditions were generated using FVCOM. FVCOM-ICM was externally coupled to simulate the fate and transport of radionuclides. Given that the ^{239}Pu is the largest fraction of the radionuclide inventory of the lagoon and Atoll islands, the model results show the highest average incremental ^{239}Pu concentration that an island may be exposed to is $3.25\text{E-}4 \text{ Bq/m}^3$ (becquerel per cubic meters), which is an increase of 84 times the average baseline/existing ^{239}Pu concentration without the storm conditions. The overall increase in ^{239}Pu average over all the islands of Atoll is about 20 folds relative to the baseline concentration. Despite the high relative increase ratios, a comprehensive exposure assessment is required to investigate the exposure risk. Further, due to the limitations of the study and uncertainties/biases in the historical data used, further research supported by field surveys to better characterize the current contamination level may be needed to make more accurate predictions.

Enewetak Atoll is in the northwest part of the Republic of Marshall Islands (RMI), approximately 4,500 km west of Hawaii (Fig. 1). The Atoll consisted of 42 islands, of which 39 still exist¹. The Atoll has been exposed to 43 nuclear tests, including the first hydrogen bomb test between 1948 and 1958^{2,3}. These tests resulted in a fallout and deposition of nuclear material to the nearby islands and marine and terrestrial environments of the Atoll, causing long-lasting nuclear contamination². A significant fraction of radionuclides from the fallout on the lagoon surface either settled rapidly to the bottom sediment of the lagoon or remained in the water column as dissolved or particle-bound material, which was eventually discharged to the Pacific Ocean^{4,5}. Although radioactive decay and environmental removal mechanisms have reduced the amounts of short-lived radionuclides (e.g., ^{54}Mn , ^{57}Co , ^{65}Zn , ^{144}Ce , ^{110}Ag , ^{95}Zr , ^{106}Ru), the lagoon sediments contain significant amounts of ^{239}Pu (Fig. 2) and small amounts of ^{241}Am , ^{240}Pu , ^{137}Cs , ^{90}Sr , ^{155}Eu , ^{125}Sb , and ^{207}Bi .

According to historical and recent studies, radioactivity associated with lagoon sediments remains the largest long-term repository of radioactive contamination at the Enewetak Atoll, with current plutonium levels 100 times or more higher than the global average^{1,7}. There is a rising concern among inhabitants in the southern islands of the Atoll and the displaced Marshallese community planning to return to the Atoll regarding the risk of resuspension of the radiologically contaminated sediments due to extreme weather events and rapid changes to global climate⁸. A typical extreme weather event for the Atoll region can be a storm or a typhoon combined with high tides and winds. Most tropical depressions and tropical storms occur between September and December, although they can occur at any time in the year. Typhoons are relatively rare but can reach Saffir-Simpson categories of 3 or 4 near the Enewetak Atoll⁵. Storm surges during the passage of tropical storms and

Pacific Northwest National Laboratory, Richland, WA, USA. [✉]email: malerajage.premathilake@pnnl.gov

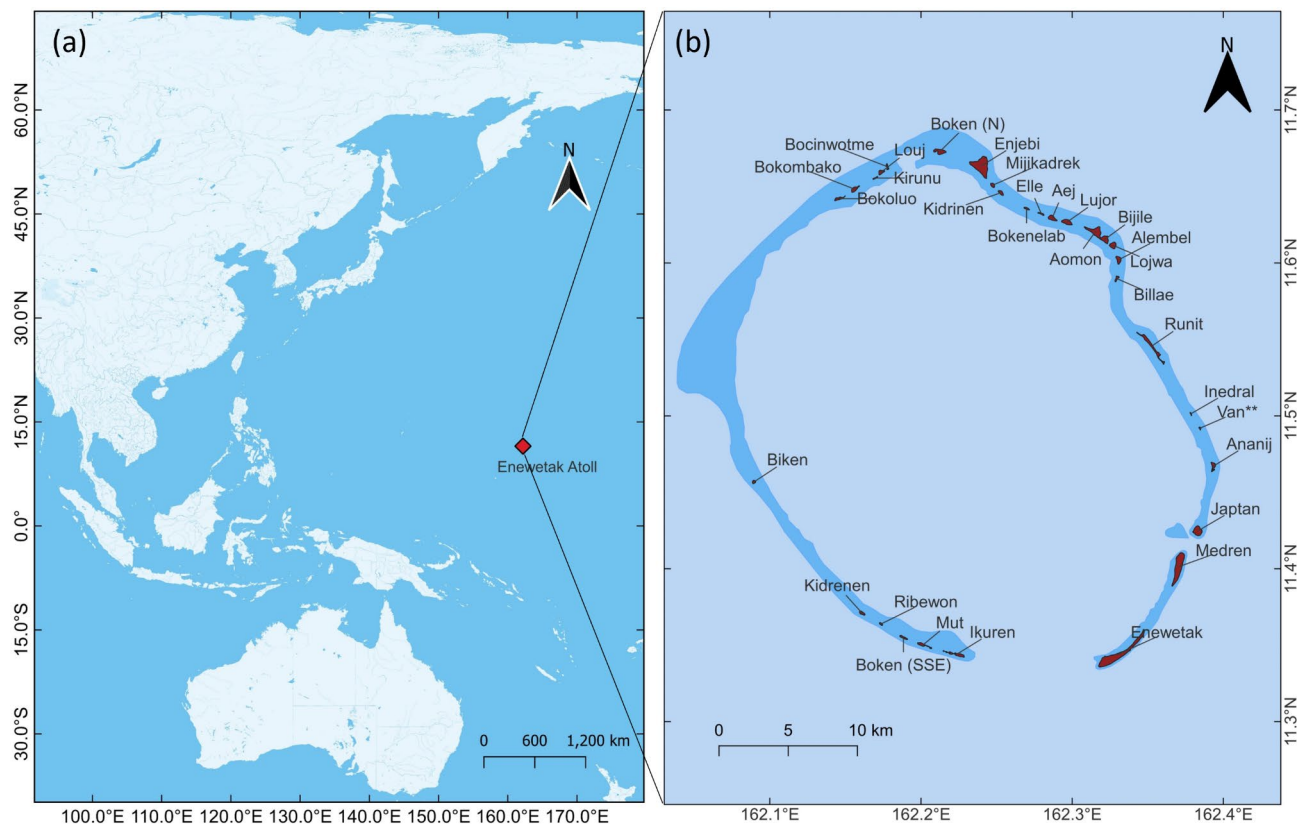


Fig. 1. (a) The geographic location of Enewetak Atoll (red colored diamond) is in West Central Pacific, and (b) The Atoll consists of 39 smaller islands with a shallow lagoon² (** this island does not have a native Marshallese name and labeled with designated US name)². The maps were created using QGIS software version 3.22 (<https://www.qgis.org/>)⁶.

typhoons, especially when combined with high tides, can cause damage to the low-lying islands of the Atoll. During a storm period, the strong winds over the sea waters exert a substantial wind-induced shear on the lagoon and surrounding ocean waters. As a result, the high bottom shear stresses may occur on the sediment bed, particularly in shallow depths, resulting in significant erosion⁹. One of the growing concerns is that eroded radionuclide-bound sediments can transport and remobilize throughout the lagoon by the currents and tides, posing an exposure risk during extreme weather events. In addition to the potential resuspension of deposited radionuclides in the lagoon's bottom sediments, the failure or collapse of the Runit Dome (located on Runit Island), which contains a substantial inventory of contaminated material, may cause further exposure risks^{9,10}. This study explores the potential impact of extreme weather events on the contamination levels in Enewetak Atoll using a numerical modeling-based approach.

Numerical modeling of storm-induced fate and transport of sediments in a coastal ocean environment is inherently complex and poses multifaceted challenges. The modeling of storms (i.e., tropical cyclones) alone presents its own unique challenges, particularly the modeling of microphysics and the intensification of storms under future warmer climates. Additionally, modeling ocean hydrodynamics under storm conditions requires considering several aspects of storm conditions, such as winds, precipitation, and waves, with high accuracy. Although the coupled storm ocean hydrodynamic modeling has not fully matured over a wide range of scales, several robust frameworks have been developed for regional-scale studies. The Weather Research and Forecasting (WRF) model with a coupled ocean modeling framework (WRF and the Regional Ocean Modeling System (ROMS)) has been used in a hindcasting study of hurricane Irene⁹. A similar WRF-ROMS coupled framework was adopted to study the tropical cyclones in the Bay of Bengal under the future climate¹¹. An integrated framework with WRF and Finite Volume Community Ocean Model (FVCOM) with the coupled Simulating WAves Nearshore (SWAN) model (FVCOM-SWAVE) was used to investigate the future storm-induced hydrodynamic conditions in the Baltic Sea¹². In addition to modeling storms and coupled ocean hydrodynamics, another modeling step is needed to evaluate the fate and transport of radionuclide-bound sediments under storm conditions. There are mature sediment transport models developed on regional scales to capture the intricate sediment processes in a coastal ocean system, including erosion, sediment suspension and deposition, aggregations, and morphological changes to sediment beds, etc. However, the dynamic and heterogeneous nature of coastal systems makes it difficult to generalize the sediment behavior across different coastal systems, and modeling requires considering site-specific features and relies heavily on site-specific data. Storm events and associated ocean hydrodynamics introduce another layer of complexity to sediment processes.

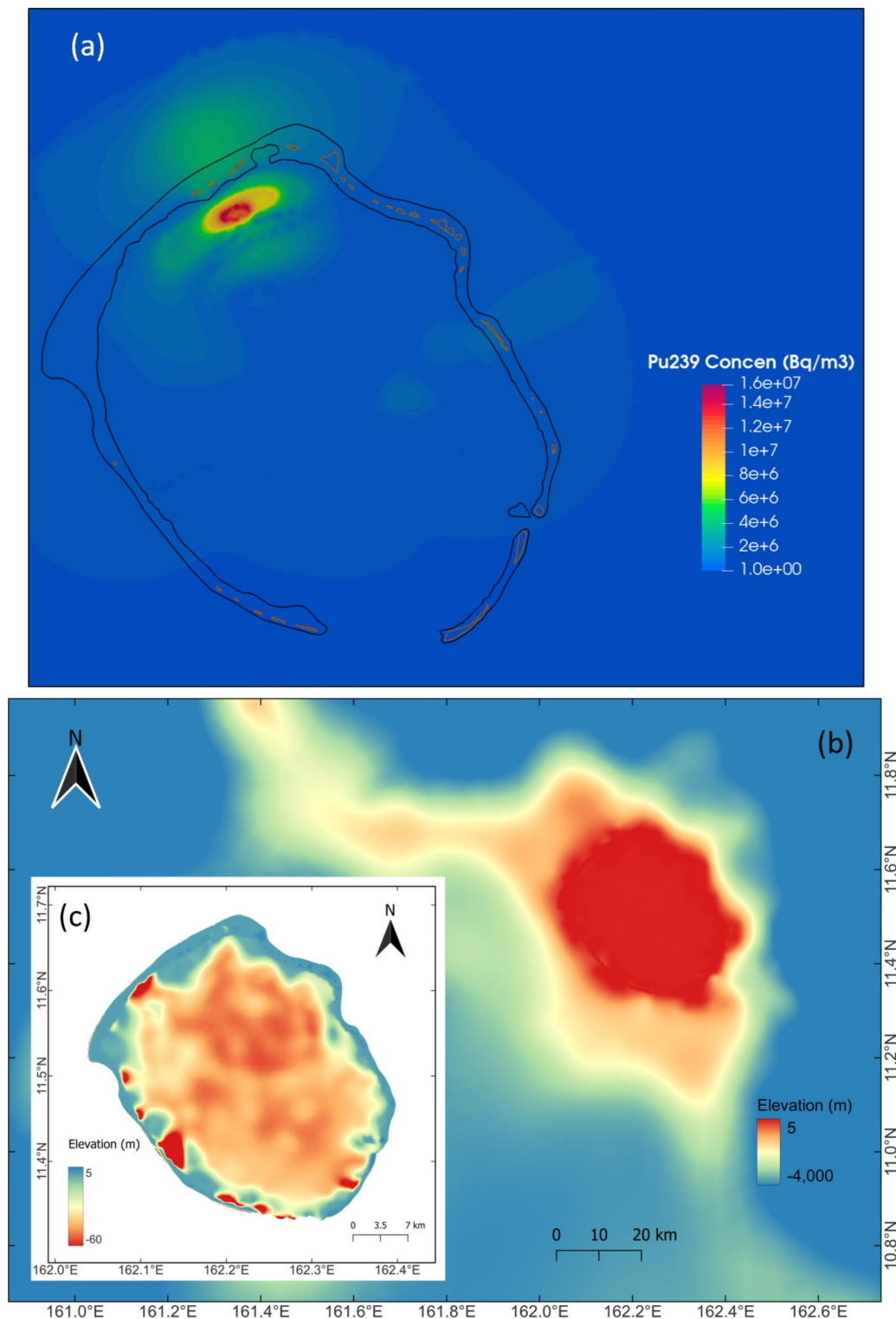


Fig. 2. (a) Estimated ^{239}Pu concentration in lagoon sediments and island soil for the year 2015². These concentrations are distributed over a depth of 50 cm in a sediment bed (supplementary material S1). (b) Depth contours of the Atoll region, including the surrounding ocean waters – The atoll is located on a volcanic seamount, and the contours show a sharp gradient of bathymetry around the atoll (c) The enlarged and rescaled depth contours of the Atoll and the lagoon showing substantial shallow water depths inside the lagoon compared to surrounding ocean.

The intensity, duration, and frequency of storms can vary significantly, and their impact on sediment transport becomes highly non-linear and pushes the mechanistic models of sediment processes to their limits^{13,14}. The Coupled Ocean–Atmosphere–Wave–Sediment Transport (COAWST)¹⁵ modeling framework is based on the combination of WRF and ROMS and was developed to simulate the storm-induced sediment transport on the east coast of the continental U.S. This study highlights the intricacies associated with the coupling of WRF, ROMS, and SWAVE models and is a promising effort to integrate the dynamic feedback between multiple model components. Similar coupled modeling frameworks^{16–18} were used to study the sediment transport under the combined effect of waves and currents. In addition to the sediment transport under physical forces, interactions between radionuclides and sediments may play a pivotal role in determining the fate and transport of radionuclides in coastal systems. The fate of radionuclides may be dictated by the ability to partition into suspended matter through sorption/desorption and radioactive decay. In addition, the secondary kinetic processes, such as progeny creations, biodegradation, etc., make the modeling fate and transport significantly complex¹⁹. Getting to operate all the three necessary components required for this modeling effort (atmospheric modeling with storms, ocean hydrodynamics, fate and transport of sediments coupled with radionuclide kinetics) on a dynamically coupled setup with a seamless data transfer is inherently complex, and the lack of site-specific data to validate each component amplifies the uncertainties associated with model results. Therefore, we adopted an approach by externally coupling WRF, FVCOM, and FVCOM-ICM to simulate the fate and transport of radionuclides associated with the lagoon sediments and Atoll's landscape. In addition to storm-induced fate and transport of radionuclides under the current climate, the analysis also investigates the compounded effect of sea level rise combined with intensified storms under future climate conditions on the potential remobilization of radionuclide-bound sediments.

Results

Storm scenarios under historical and future climates

The simulated historical storm scenarios used for the analysis are shown in Fig. 3. The three selected storms were simulated using WRF-ARW²⁰, with a single domain at a horizontal grid spacing of 9 km and the storm-induced meteorological conditions for the region, including the Atoll, were reproduced. The selection of storms and modeling approach is described in “Methodology,” and additional details are provided in the supplementary material. Figure 3 shows the comparison of predicted storm tracks (red line) and intensities (colored dots on track) against the observed tracks (black line) and intensities. Storms 1 and 3 were simulated reasonably well. Because of the unusual observed track of Storm 2, WRF-ARW could simulate the storm with reasonable accuracy for the initial few days but deviated above 35°N, which was farther away from the Enewetak Atoll. The marginal differences in the intensities can be attributed to the uncertainties and biases associated with model-forcing data and physical parameterizations.

The corresponding future storms were simulated with the perturbed future climate conditions using pseudo-global-warming (PGW) method⁵. Due to the high variability of future climate predictions by different General Circulation Models (GCMs) and their sensitivity to sea surface temperature (SST), atmospheric temperature, and humidity, we utilized an approach to derive the future storm conditions based on the multi-model ensembles⁵ (supplementary material S2.2). Figure 4 shows potential tracks and intensities for Storm 3 under perturbed future climate year 2090. The predicted tracks and intensities show less variation close to the island and surrounding region and exhibit a significant divergence in storm path and differences in intensities as the storm propagates.

Figures 5, 6 show the simulated storm tracks and corresponding wind velocities for storms 1 and 3. Storm 1 under the future climate (year 2090) shows lower wind compared to wind speeds under the current climate. Although Storm 3 shows a low wind speed under future climate compared to the current climate conditions, future Storm 3 exhibits a rapid intensification as it propagates towards the western Pacific⁵. A high emphasis was placed on Storms 1 and 3 due to their relatively high strength and proximity to the Atoll compared to Storm 2.

Ocean hydrodynamics under storm conditions

Being a shallow lagoon located on a sea mount, Enewetak Atoll exhibits hydrodynamics and circulation patterns primarily driven by tides and winds. One of the measures that indicates the quality of the marine waters of the lagoon is residence/flushing time. The residence time of the Atoll's lagoon is approximately one-month estimated by studying the volumetric transport patterns²¹. We conducted a numerical dye (a passive tracer) study in the lagoon by initializing the lagoon volume with constant dye concentration (1.0 mg/L) and simulated the fate of the dye under regular tides and meteorological conditions of the current year 2015 without storms, which was considered as the baseline conditions. Our numerical dye study also shows that the e-folding flushing time²² of the lagoon is around 30 days (Fig. 7). Although the estimated bulk flushing time is 30 days for the lagoon volume, high residual tracer concentrations have sustained around the shallow island areas even after 30 days (Fig. 8), partly because the ocean model considered the atoll islands as part of the water domain and has been initialized with tracer concentration. Since the main source term for the study was deposited sediments in the lagoon, water circulation in the lagoon dictates the residence time; we used the estimated e-folding flushing time as the transport time scale to determine the simulation duration for fate and transport scenarios described in the next sections. The intensified winds and the tidal conditions induced by the storms alter the baseline/existing hydrodynamic conditions of the lagoon waters. Particularly, the high wind exerts a substantial wind-induced shear on the lagoon waters while amplifying wave-induced flooding. Figure 9a–d shows the propagation of the wind field during Storm 1, which was generated by WRF-ARF and then used in the FVCOM model setup to generate hydrodynamics and circulation in and around the Atoll. The impact of the wind field on the lagoon water depends on the proximity of the storm track, the radius of maximum wind, and the timing and orientation of the wind field.

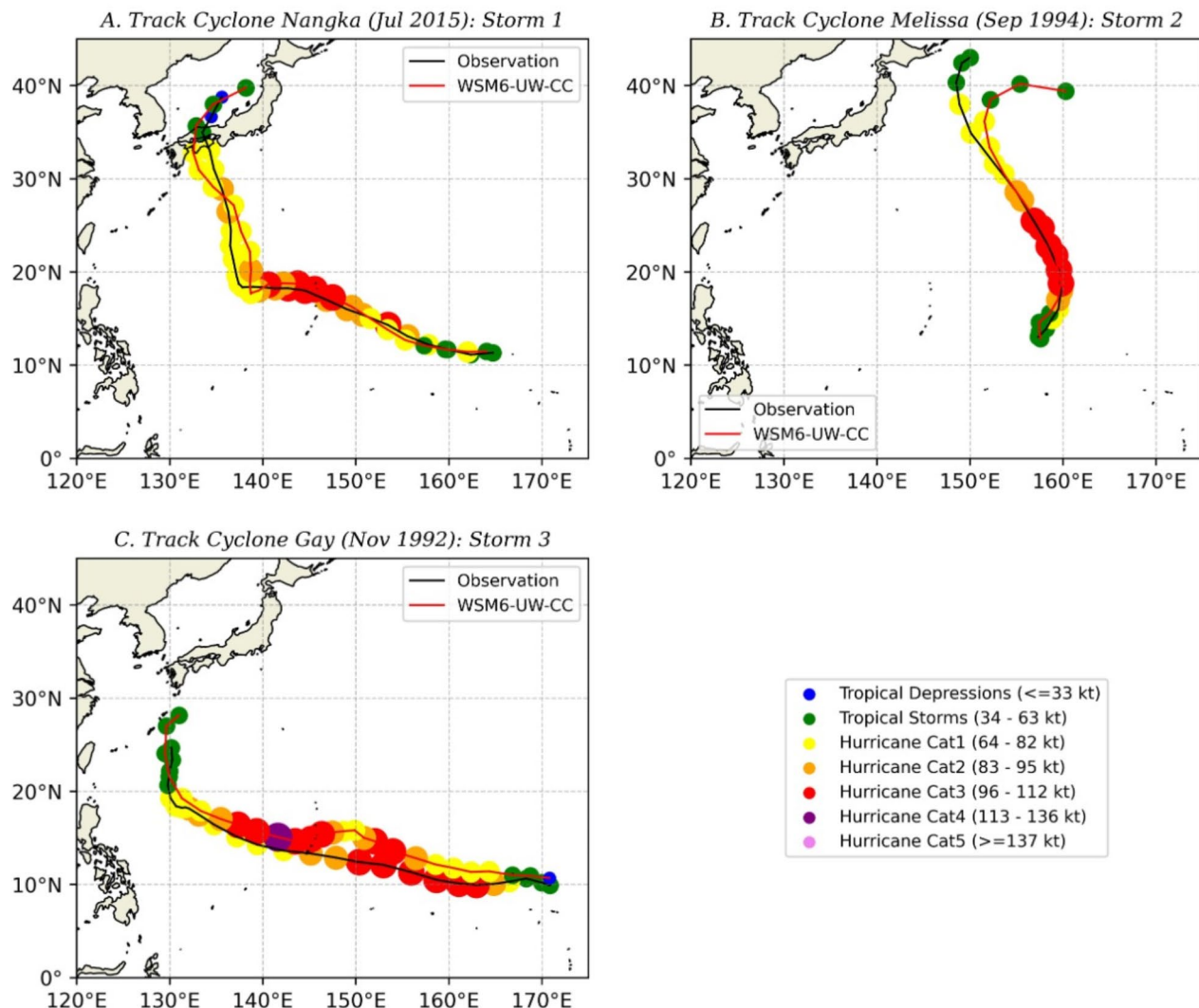


Fig. 3. Simulated vs. observed storm tracks for selected historical storms close to Enewetak Atoll. (A) Storm 1 - occurred in July 2015 (B) Storm 2 - occurred in September 1994 (C) Storm 3 - occurred in November 1992.

Figure 9e-g shows the variation of ocean surface currents as the storm travels in close to the Atoll. The shallow areas of lagoon waters exhibit a significant increase in surface water currents during the phase in which the Atoll is exposed to the maximum wind effect induced by the storm, resulting in higher bottom shear stresses and increasing the likelihood of resuspension of radionuclide-bound sediments deposited in the shallow regions. However, the wind shear-induced high bottom stresses last for a shorter duration (2–4 h), and the effect is transient. Figure 10 shows the variation of maximum bottom shear stress during the storm periods, which also indicates that the high bottom shear exists for a short time span that may result in potentially heavy bottom erosion.

Mobilization and transport of radionuclides

The fate and transport of the resuspended radionuclide-bound sediments is primarily dictated by the ocean current field. Given the existence of background radionuclide concentration (i.e., The term “concentration” has been used to denote the volumetric activity concentration) associated with suspended sediments already in the lagoon and surrounding waters due to the erosion and settling processes, which are in dynamic steady state under regular tides and currents, the study focused on estimating the incremental radionuclide concentration during the storms under the current and future climates. Although we simulated the fate and transport of six radionuclides (^{241}Am , ^{239}Pu , ^{137}Cs , ^{90}Sr , ^{155}Eu , and ^{125}Sb), the results were presented only for ^{239}Pu and ^{137}Cs which are the larger fractions of the total radionuclide inventory in bottom sediments (Fig. 2) compared to other radionuclides.

Selected Tracks in Current and Future Climate for Storm 3

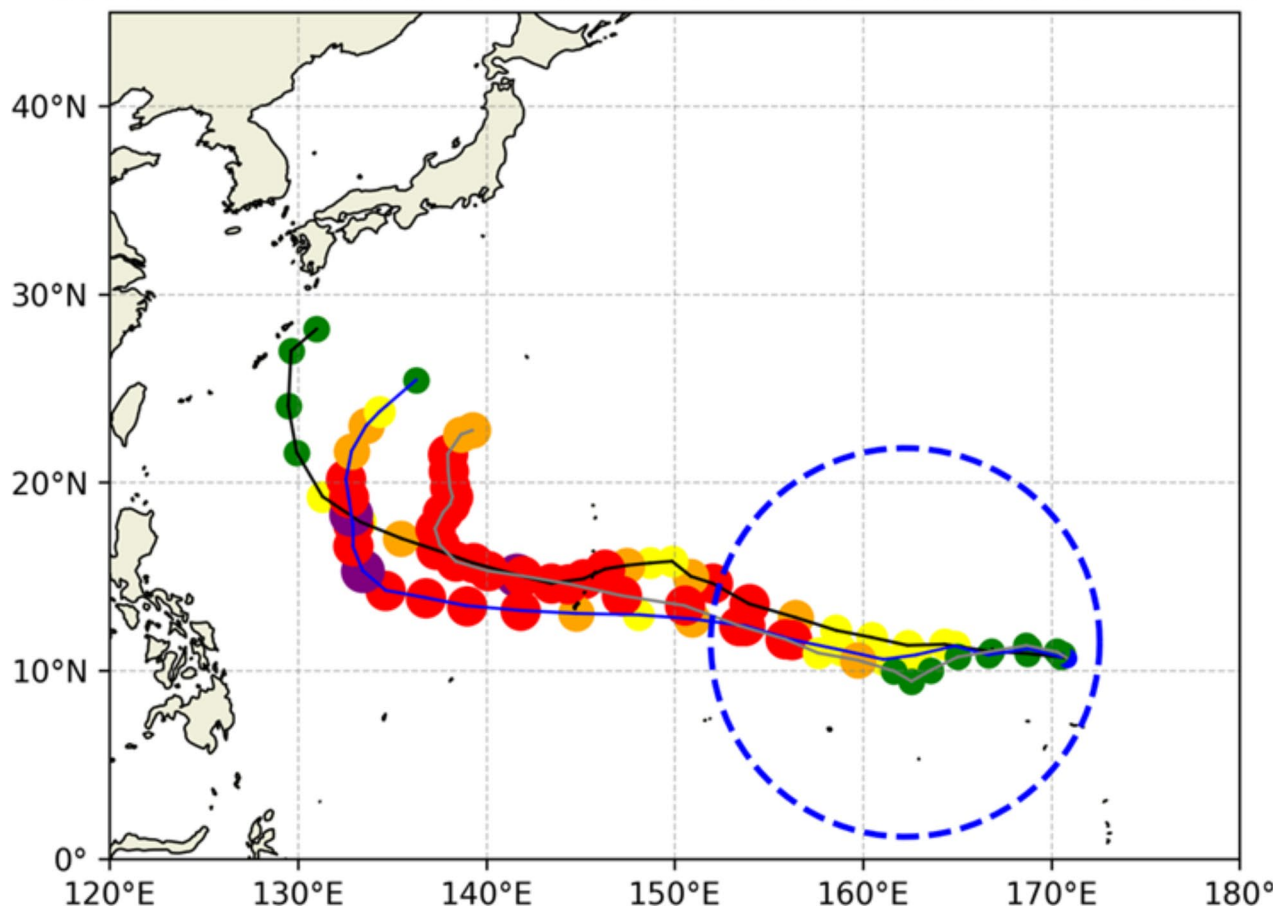


Fig. 4. WRF-ARW simulated storm tracks of Storm 3 in the current climate (black) and in the future climate using MIRROC6 perturbations (blue). The 11-member ensemble mean storm track is also shown (gray). The dots along the storm tracks are plotted every 12 h.

Fate and transport under baseline conditions

The changes in the radionuclide concentrations due to the combined effect of erosion and settling under the regular tides and ocean currents without storm conditions (baseline scenario) are presented in Figs. 11, 12. The baseline scenarios were simulated for a 30-day period for both current year (2015) and future year (2090) without imposing storm conditions as the reference benchmark for radionuclide activity under normal oceanic and meteorological conditions. Figure 11 shows the maximum concentration distribution of ^{137}Cs in the surface layer of the lagoon. The ^{137}Cs distribution patterns in both current and future years have shown qualitatively similar overall extent (Fig. 11a,b). The differences seen between current and future years can be attributed to radioactive decay. The bottom sediment has lower ^{137}Cs concentration in the future year compared to the current year due to the radioactive decay resulting lower ^{137}Cs activity in the resuspended sediments in the future year. Figure 11 also depicts that the northern islands and nearby waters show the highest maximum ^{137}Cs concentration primarily due to the large inventory of radionuclide concentrations accumulated in the sediments as a result of the fallout from the historical nuclear tests. In contrast to ^{137}Cs , the surface concentration maps of ^{239}Pu show (Fig. 12) overall minimum differences in maximum concentrations for the current and future years due to the longer half-life of ^{239}Pu compared to ^{137}Cs producing negligible radioactive decay. Also, the minor differences in ^{239}Pu distribution in Fig. 12 for the current and future years are affected by the forcings associated with the future climate, such as sea level rise (supplementary material S2.1) and other meteorological conditions (e.g. wind, air pressure, humidity, precipitation, solar radiation).

Fate and transport under storm conditions

During storm events, the wind-induced high bottom shear stresses have the potential to cause higher levels of erosion⁹ resulting in potentially high radionuclide concentrations in the water column. However, the compounded effect of wind-induced bottom shear intertwined with regular tides-driven bottom shear can generate highly non-linear combined effects. Figure 13 shows the comparison between the maximum ^{137}Cs distributions in the surface layer for current and future years under Storm 1 conditions. The peak concentration

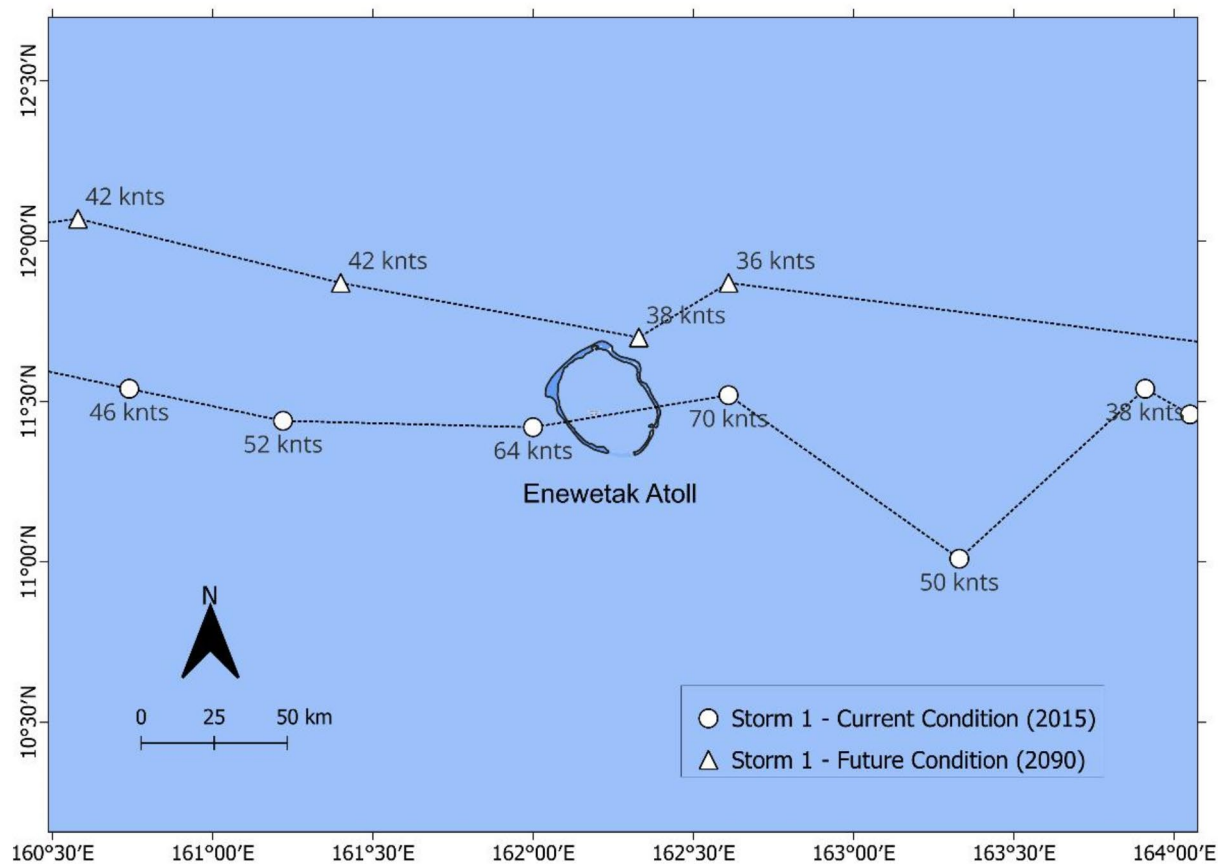


Fig. 5. The simulated pathways and wind speeds of Storm 1 with close proximity to Atoll under current climate (2015) and future climate (2090). The data for historical storms was obtained from the International Best Track Archive for Climate Stewardship (IBTrACS) database (<https://ncics.org/ibtracs/>).

of ^{137}Cs for the current year is higher than the future year, which is partially due to the lower concentration of ^{137}Cs in the bottom sediments in future years because of radioactive decay.

The other contributing factor for the significantly lower peak concentrations in the future compared to the current year is the substantial reduction in the intensity of Storm 1 in the future (Fig. 5), resulting in a lower wind-induced shear on lagoon waters. The effect can be further compounded by the shifting of the path of Storm 1 away from the lagoon. Further, a comparison between Figs. 11, 13 indicates that, under Storm 1, there is a potential for the plume of suspended radionuclides to extend the intrusion into the lagoon and spread further towards the southern islands under the current climate compared to the future year.

Despite being affected insignificantly by the decay process in future year (2090), ^{239}Pu also shows noticeably low peak concentrations in the bottom layer, where the immediate effect of erosion is expected during Storm 1 period (Fig. 14), which indicates the future distribution is greatly impacted by the weakening of the strength of Storm 1 in the future year.

In comparison to Storm 1, Storm 3 has higher strength, and the trajectories for both current and future years lie to the south of the Atoll (Figs. 5, 6). However, the lagoon waters can be substantially affected by the strong winds from Storm 3, as the Atoll is within the radius of maximum wind. Figure 15 shows the peak concentrations of ^{137}Cs in the surface and bottom layers for Storm 3 periods of current and future years. In comparison to Storm 1 scenario, Fig. 15 shows an increase in peak concentration distributions for both current and future year, indicating a higher wind-induced erosion under Storm 3. Figure 16 shows the peak concentrations of ^{239}Pu distribution in the bottom layer for Storm 3 period and a noticeable increase in peak concentration in comparison to Storm 1.

The Figs. 13, 14, 15, 16 provide the spatial distribution of the maximum potential activity (i.e., peak concentrations) that may occur during the storms and post-storm periods. However, the peak concentrations are transient and do not reflect the exposure concentrations that the islands and their inhabitant may be exposed to during a potential storm period due to the increased activity concentration in the surrounding seawater. To understand the levels of incremental concentration caused by the storm-induced hydrodynamics, we analyzed the average radionuclide concentrations that each island is exposed to (i.e., activity concentration received to

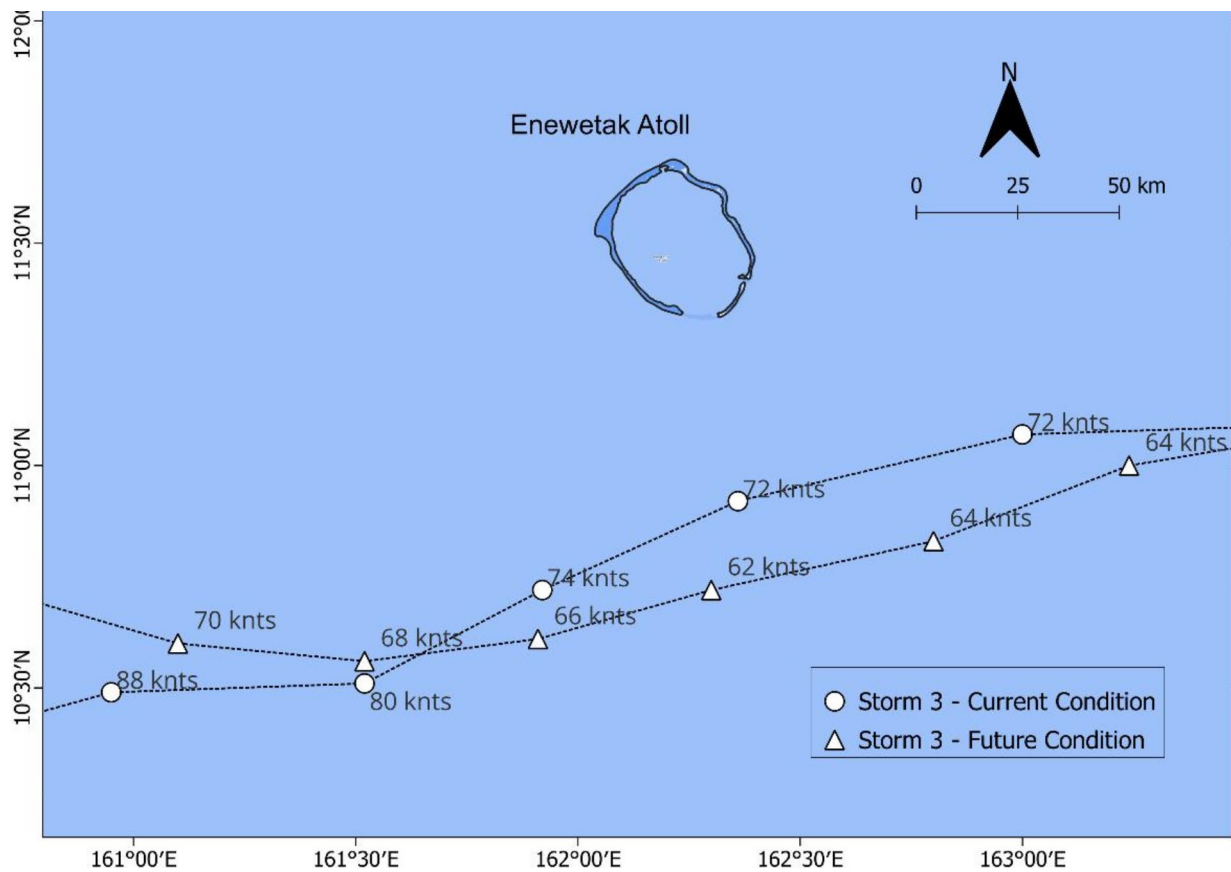


Fig. 6. The simulated pathways and wind speeds of Storm 3 with close proximity to Atoll under current climate (2015) and future climate (2090). The data for historical storms was obtained from the International Best Track Archive for Climate Stewardship (IBTrACS) database (<https://ncics.org/ibtracs/>).

the surrounding waters of the island) during each storm event (30 days). The concentrations from the fate and transport simulations were temporally averaged over a 30-day period and spatially averaged over a domain around each island limited to a water depth of 2 m, which includes the receptor points (supplementary material S4.3). Figures 17, 18 show the distribution of average ^{239}Pu concentrations that each island is exposed to under baseline and storm conditions for current and future climates, respectively.

Here, ^{239}Pu was selected as the representative radionuclide to infer the overall remobilization pattern, as ^{239}Pu is an isotope with a very long half-life, and it is the largest fraction of the estimated radionuclide inventory of the lagoon. The northern island group, located close to a region where the bottom sediments contain a significantly high inventory of ^{239}Pu , exhibits the highest concentration during Storm 3 under the current climate, reaching up to 4 to 5 times the corresponding baseline/existing averaged ^{239}Pu concentrations.

This is partially caused by the higher strength of Storm 3 as well as the alignment of the wind field where the ^{239}Pu hot spot is located with a sufficient distance to exert the maximum wind shear. However, the overall increase of activity due to the remobilization of radionuclide-bound sediments is significantly higher around the islands located in the Northeastern and Southern parts of the Atoll during the storm periods under the current climate. This indicates the high probability of eroded contaminated sediments from northern parts of the Atoll being transported to Northeastern and Southern regions by the water circulation. This increase can be significant around the islands located in the northeastern part, reaching an increase in existing (baseline) activity by a factor of 84. The predicted ^{239}Pu concentrations during storm periods under future climate (Fig. 18) show a different distribution pattern, indicating a reduction of exposure concentrations for several islands, mainly during Storms 1 and 2. This may be attributed to the weakening of Storms 1 and 2 while traveling close to the Atoll under the future climate and the non-linear ocean circulation patterns caused by the compounded effect of storm forcing coupled with tidal currents of lagoon waters and sea-level rise in shallow areas. Figure 19 shows the model predicted future ^{239}Pu concentrations during the storm events while simultaneously considering the release of radiologically contaminated sediments buried in the Runit Dome. Given that ^{239}Pu is the largest fraction of inventory inside the Dome²³, Fig. 19 shows noticeably increased potential future concentrations compared to the future prediction without Dome collapse indicating the potential risk of such an event.

Methodology

The existing literature describes the history of nuclear tests at Enewetak Atoll, cleanup, and remediation efforts, and attempts to characterize the extent of contamination by assessing the inventory of remaining radionuclides

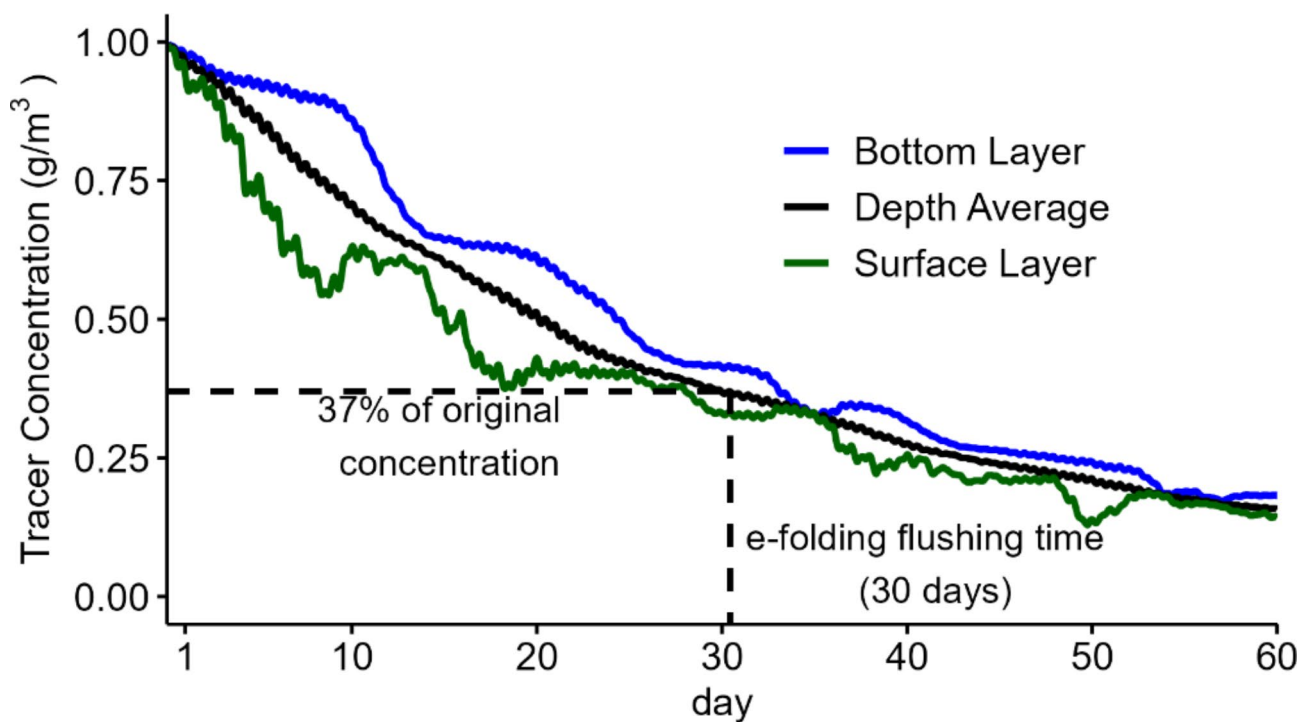


Fig. 7. The variation of numerical dye (passive tracer) concentration in the water column over time, which was introduced to the lagoon water over the full volume with an initial concentration of 1 g/m^3 under baseline conditions. Here, the surface (green line) and bottom (blue line) layers are the uppermost and bottommost layers of the terrain following the sigma coordinate layers used in the ocean model (supplementary material S3.1). The e-folding flushing time was used as the transport time scale for any contaminant introduced into the lagoon water instantaneously.

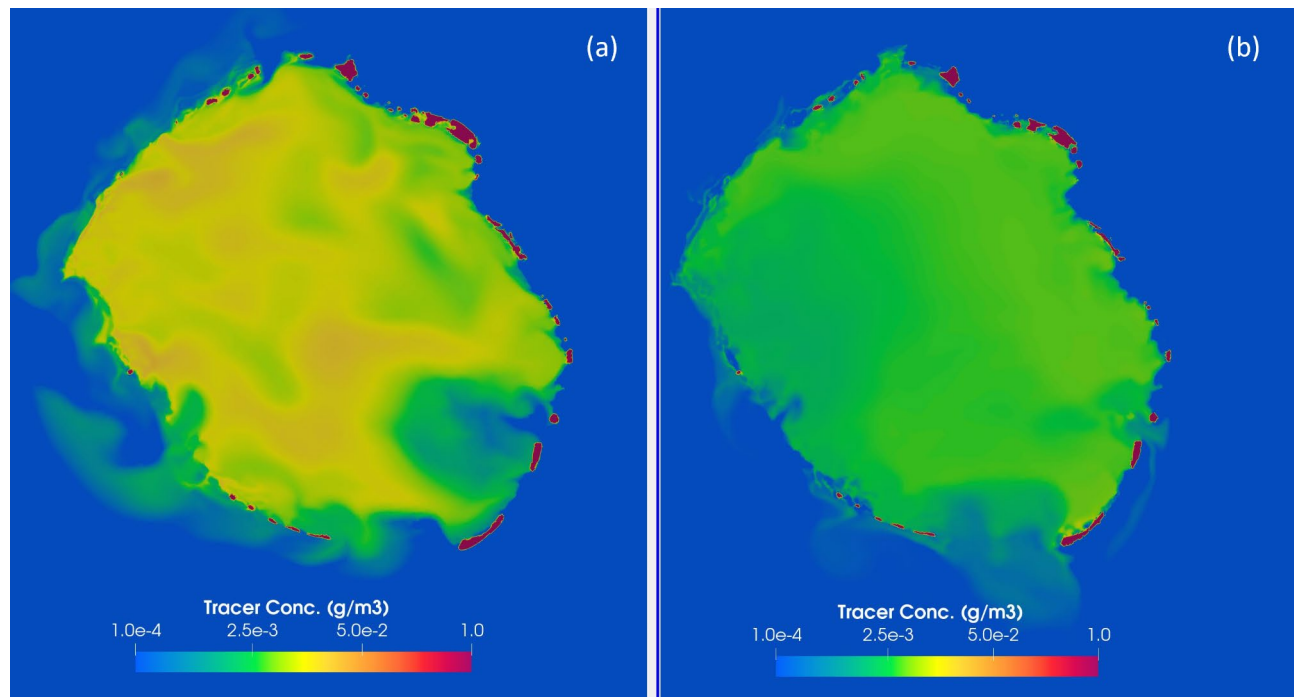


Fig. 8. The distribution (color are in logarithmic scale) of numerical dye (tracer) in the surface layer (uppermost layer of terrain following sigma coordinate layers used in the ocean model) under baseline conditions of the current year (2015) (a) after one day (b) after 30 days.

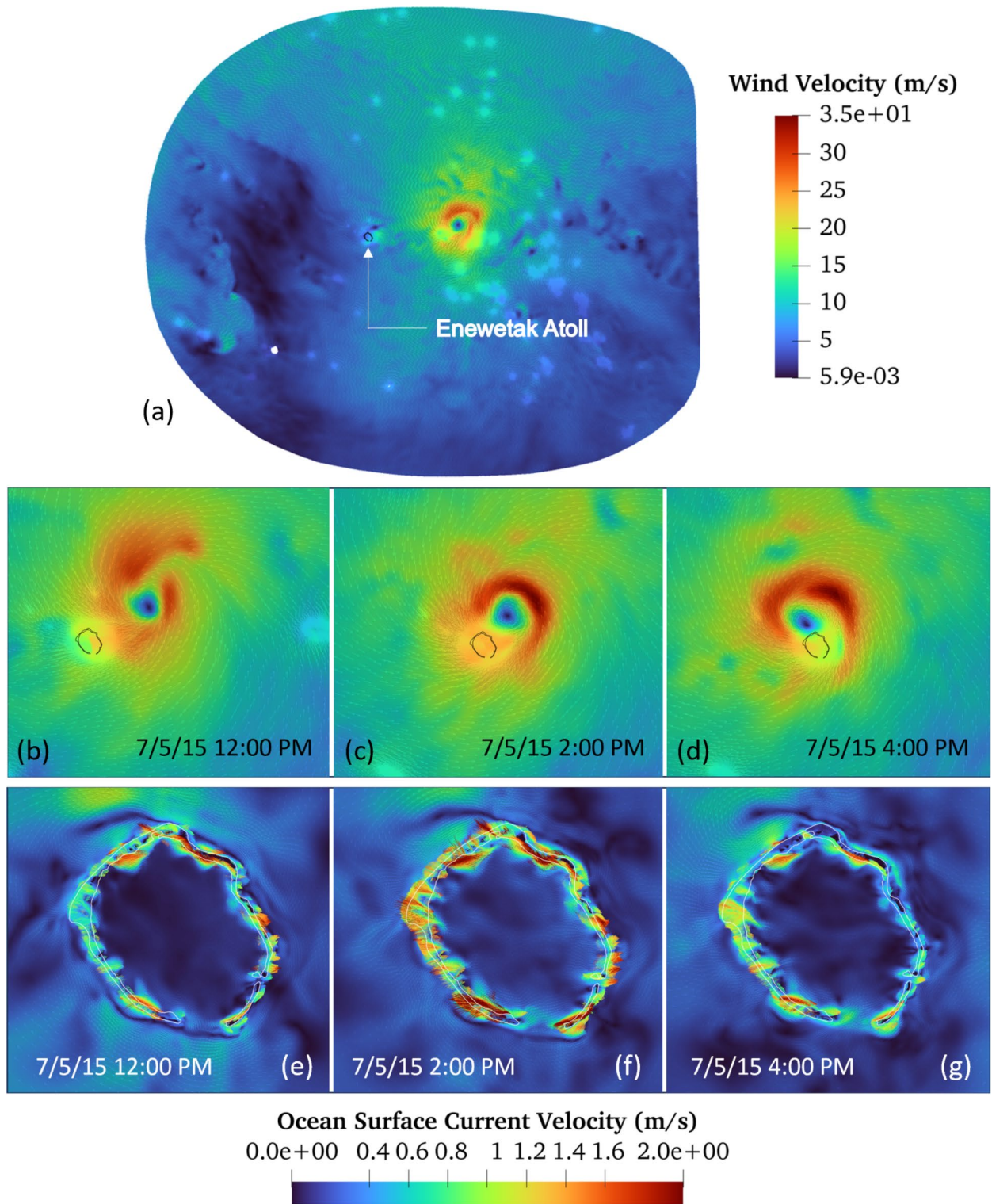


Fig. 9. The storm-induced wind shear during Storm 1 and its impact on ocean surface currents (a) The instantaneous wind field during Storm 1 under the current climate is visualized over the computational domain. This figure shows a snapshot of the progression of the storm when it is building up from a distance east to the atoll. (b, c) The propagation of the instantaneous wind field during Storm 1 under the current climate at selected time windows (snapshots) when it travels close to the Atoll (e–g) The corresponding variation of ocean surface currents induced by the winds shear during Storm 1 progress under the current climate.

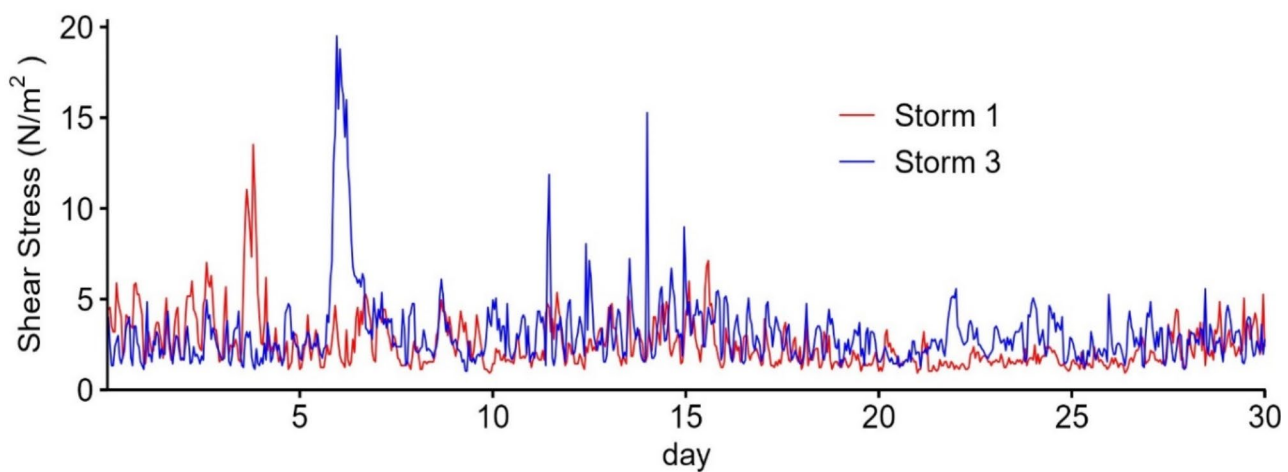


Fig. 10. The model variation of the predicted maximum shear stress in the bottom water layer that exerts on the sediment bed during the 30-day storm simulation period for Storm 1 and 3 under the current climate. The large peaks are attributed to the short time span that the storms exert the greatest wind shear.

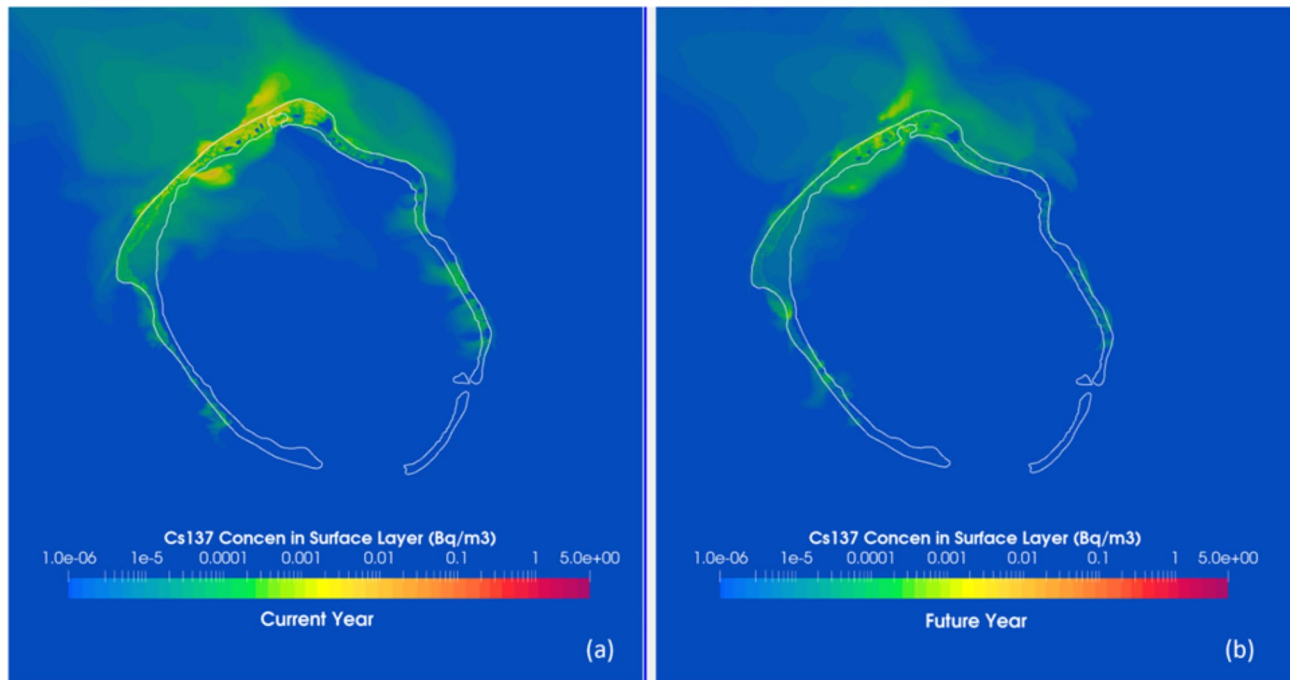


Fig. 11. The distribution of maximum total ^{137}Cs concentration (sum of dissolved and particulate forms) in the surface layer (the uppermost layer of the terrain following sigma layers of the ocean model starting from the ocean water surface) of the lagoon and surrounding waters for the baseline scenario under (a) current (2015) and (b) future (2090) climate conditions.

in the environment. Historical surveys^{2,7} have characterized the radionuclide concentrations in lagoon sediments and waters and islands in detail. The modeling analysis was conducted for two selected years: (1) current year – 2015, (2) future year – 2090. The selection of the current year was partially based on the availability of data requirements for climate modeling and also partially influenced by a notable historical storm that occurred in July 2015 in close proximity to the Atoll. In order to correctly represent the contamination levels in the bottom sediment and land soil for current and future years, the radionuclide concentrations surveyed in the historical years were corrected with radionuclide decay, neglecting the biodegradation (i.e., degradation of activity concentration due to biological processes in a marine system)²⁴ or other depuration mechanisms.

Regional climate modeling over the western Pacific Ocean, particularly in proximity to RMI, is limited. Although global climate models offer comprehensive coverage of the broader region, fine-scale regional climate

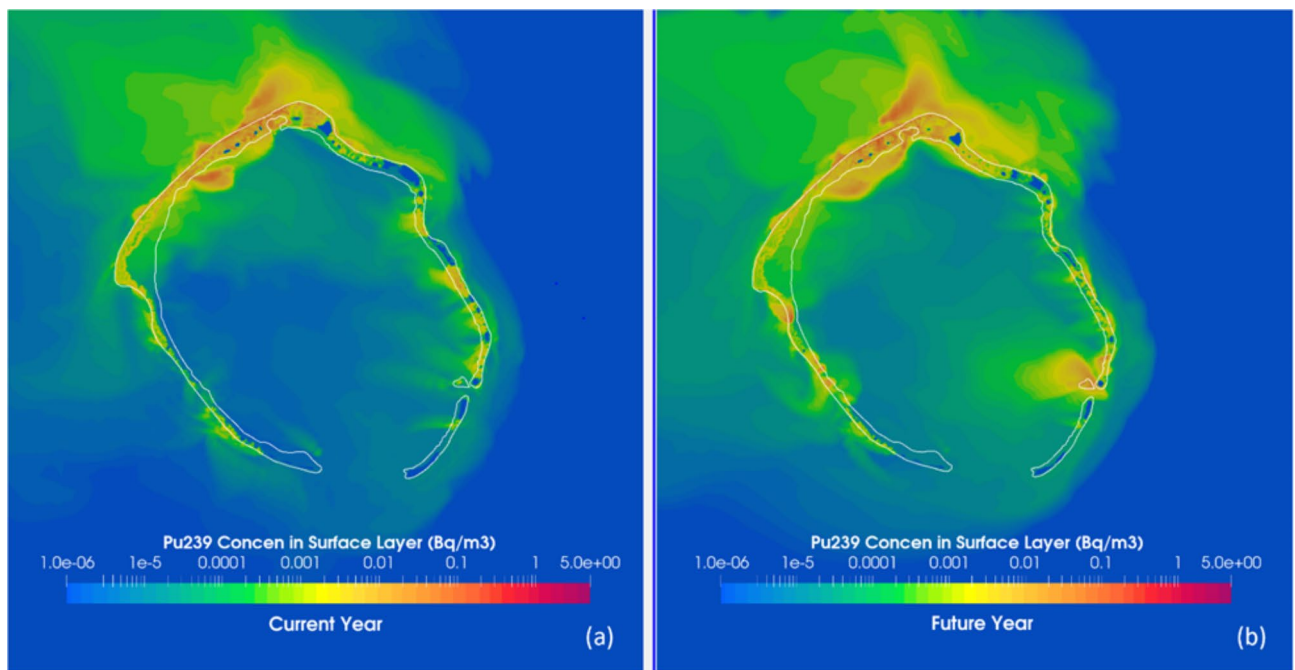


Fig. 12. The distribution of maximum total ^{239}Pu concentration (sum of dissolved and particulate forms) in the surface layer (the uppermost layer of the terrain following sigma layers of the ocean model starting from ocean water surface) of the lagoon and surrounding waters for the baseline scenario under (a) current (2015) and (b) future (2090) climate conditions.

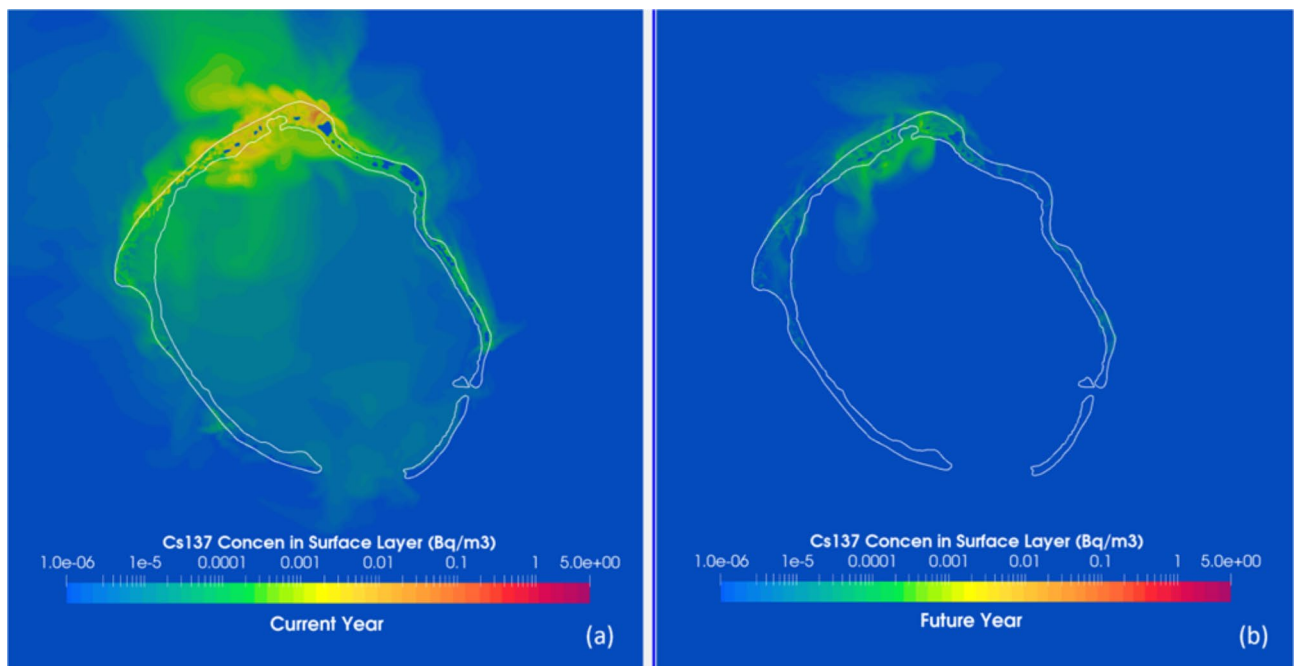


Fig. 13. The distribution of maximum total ^{137}Cs concentration (sum of dissolved and particulate forms) in the surface layer (the uppermost layer of the terrain following sigma layers of the ocean model starting from ocean water surface) of the lagoon and surrounding waters for the Storm 1 scenario under (a) current (2015) and (b) future (2090) climate conditions.

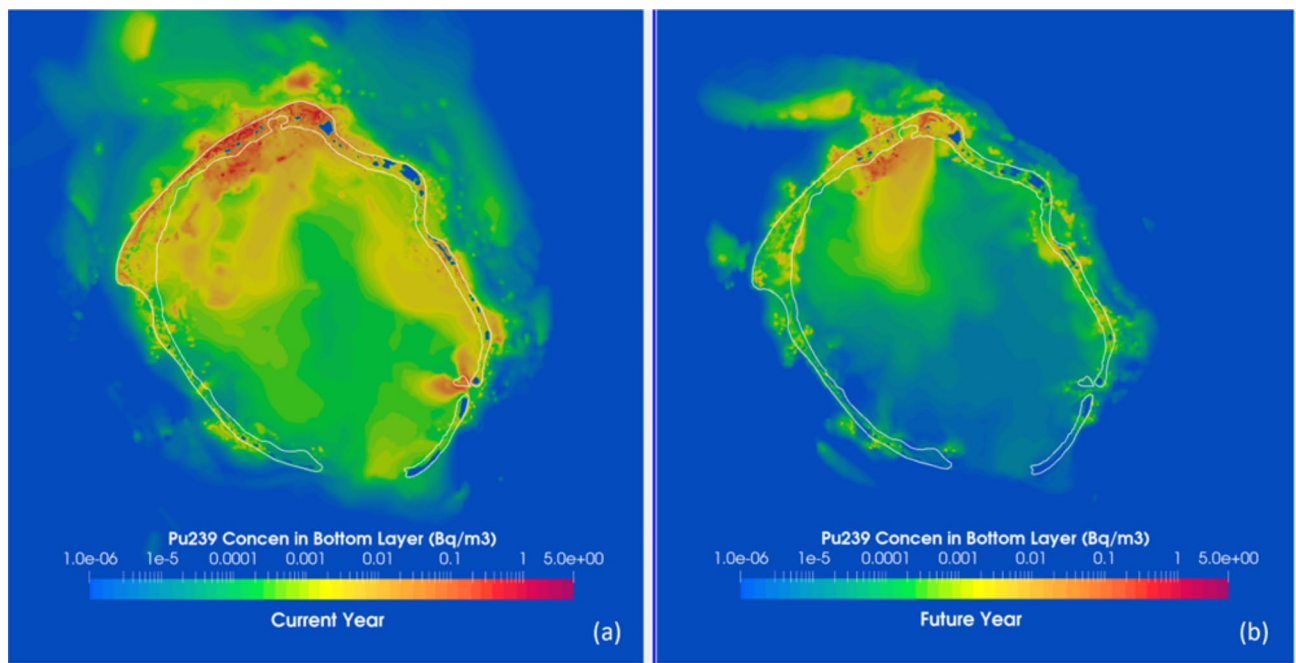


Fig. 14. The distribution of maximum total ^{239}Pu concentration (sum of dissolved and particulate forms) in the bottom layer (the bottommost layer of the terrain following sigma layers of the ocean model starting from ocean water surface) of the lagoon and surrounding waters for the Storm 1 scenario under (a) current (2015) and (b) future (2090) climate conditions.

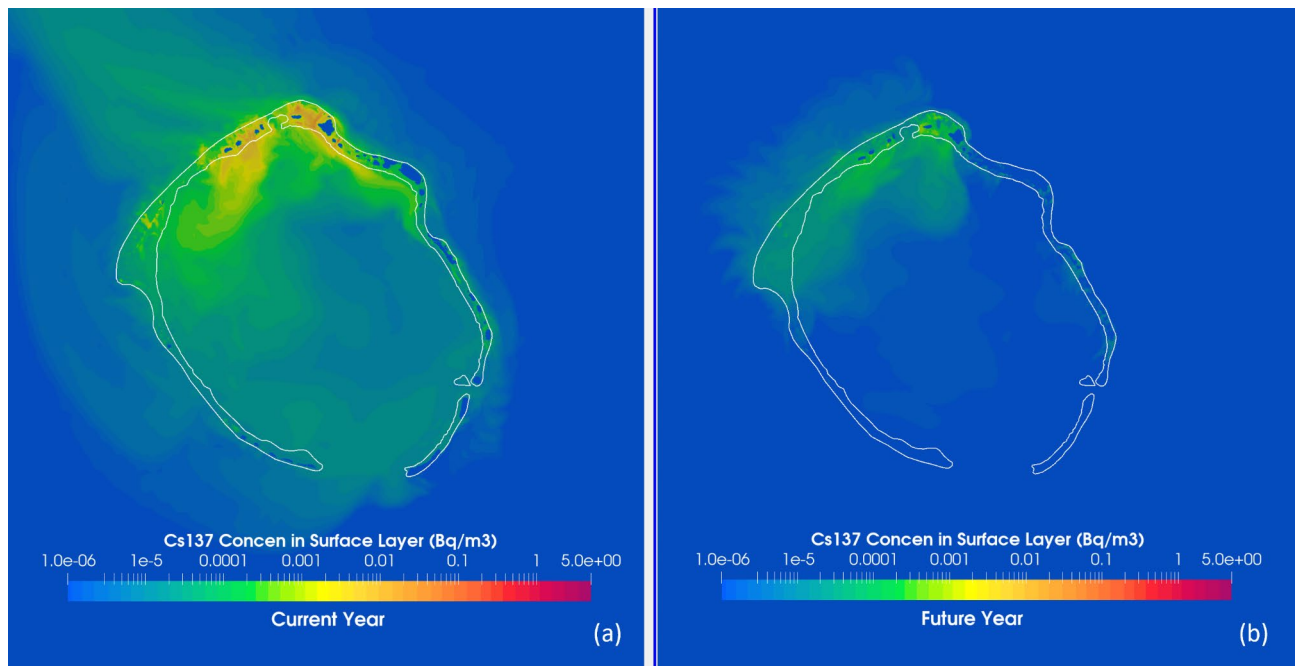


Fig. 15. The distribution of maximum total ^{137}Cs concentration (sum of dissolved and particulate forms) in the surface layer (the uppermost layer of the terrain following sigma layers of the ocean model starting from ocean water surface) of the lagoon and surrounding waters for Storm 3 scenario under (a) current (2015) and (b) future (2090) climate conditions.

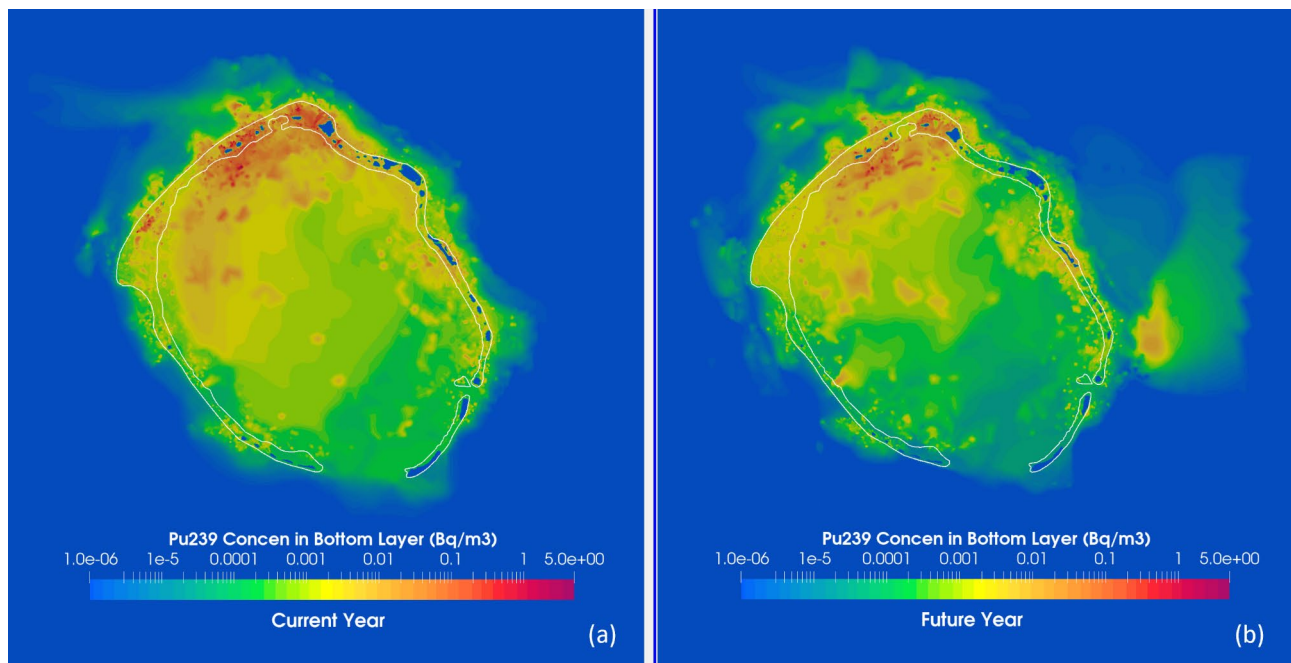


Fig. 16. The distribution of maximum total ^{239}Pu concentration (sum of dissolved and particulate forms) in the bottom layer (the bottommost layer of the terrain following sigma layers of the ocean model starting from ocean water surface) of the lagoon and surrounding waters for Storm 3 scenario under (a) current and (b) future climate conditions.

predictions for the RMI region are not available. Therefore, an independent assessment was conducted to explore and characterize the potential storms in the vicinity of the Enewetak Atoll by leveraging historical storm databases, and three historical storms were selected. These selections were based on their strength and proximity to the Enewetak Atoll, making them likely candidates to produce the most significant impact on the Atoll's environment. We employed the Advanced Research Weather Research and Forecasting (WRF-ARW) Model²⁰ to conduct simulations for both current (Y2015) and future (Y2090) climates. These simulations provided the necessary meteorological conditions for the subsequent ocean modeling scenarios. To simulate the storm-induced ocean hydrodynamics, we set up an ocean model for the RMI region using the Finite Volume Coastal Ocean Model (FVCOM)²⁵. The model domain covered almost the entire RMI Exclusive Economic Zone (EEZ), including areas within 1,000 km from Enewetak Atoll. The ocean model was driven by the storm scenarios simulated by the WRF-ARW model⁵. The FVCOM simulations provided the ocean hydrodynamic conditions for the fate and transport modeling of radionuclides.

The mobilization and transport of radionuclides in and around the lagoon were simulated using the FVCOM-Integrated Compartment Model (FVCOM-ICM)^{26,27}. FVCOM-ICM is a FVCOM framework-based biogeochemical model with mature capabilities of simulating the advection and diffusion of pollutants/contaminants^{27,28}. The radionuclide kinetics implemented in FVCOM-ICM include radioactive decay and partitioning onto suspended particulate matter (supplementary material S4.2). The primitive mechanistic understanding-based sediment processes implemented in the radionuclide kinetic module are adopted from the approach used to study the radionuclide (^{137}Cs) fate and transport in coastal ocean waters near the site of Fukushima Dai-ichi nuclear plant²⁹. However, the sedimentation-related parameterization in this approach was improved here (supplementary material S4.2) to better emulate the conditions that may arise in the lagoon⁵. Two independent baseline scenarios were conducted for the current and future years without storm conditions to assess the level of incremental radionuclide concentrations under storm conditions. In addition to the model scenarios with source terms being deposited radionuclide-bound sediments in the lagoon and soil on land, we simulated a model scenario with a hypothetical release of radionuclide inventory buried in Runit Dome. We considered a postulated instantaneous collapse/failure of the Runit Dome and distributed the total inventory on the nearby land and shoreline as a distributed pattern of a plume. (supplementary material S4.4). The radionuclide concentrations in lagoon water and sediments produced by the FVCOM-ICM simulations were analyzed, and the distributions of radionuclide activity concentrations in and around the Atoll were presented.

Limitations of the study

Despite the extensive modeling effort by the external coupling of three individual models, the final results may be constrained by (1) the uncertainties and biases in the historical assessments of radionuclide contamination, (2) the lack of data to validate the current year contamination level in the lagoon; (3) the lack of data to validate the modeled sedimentation processes in the lagoon and the surrounding waters; (4) limitations in characterizing and reproducing physical processes associated with storm induced atmospheric and oceanic conditions. The

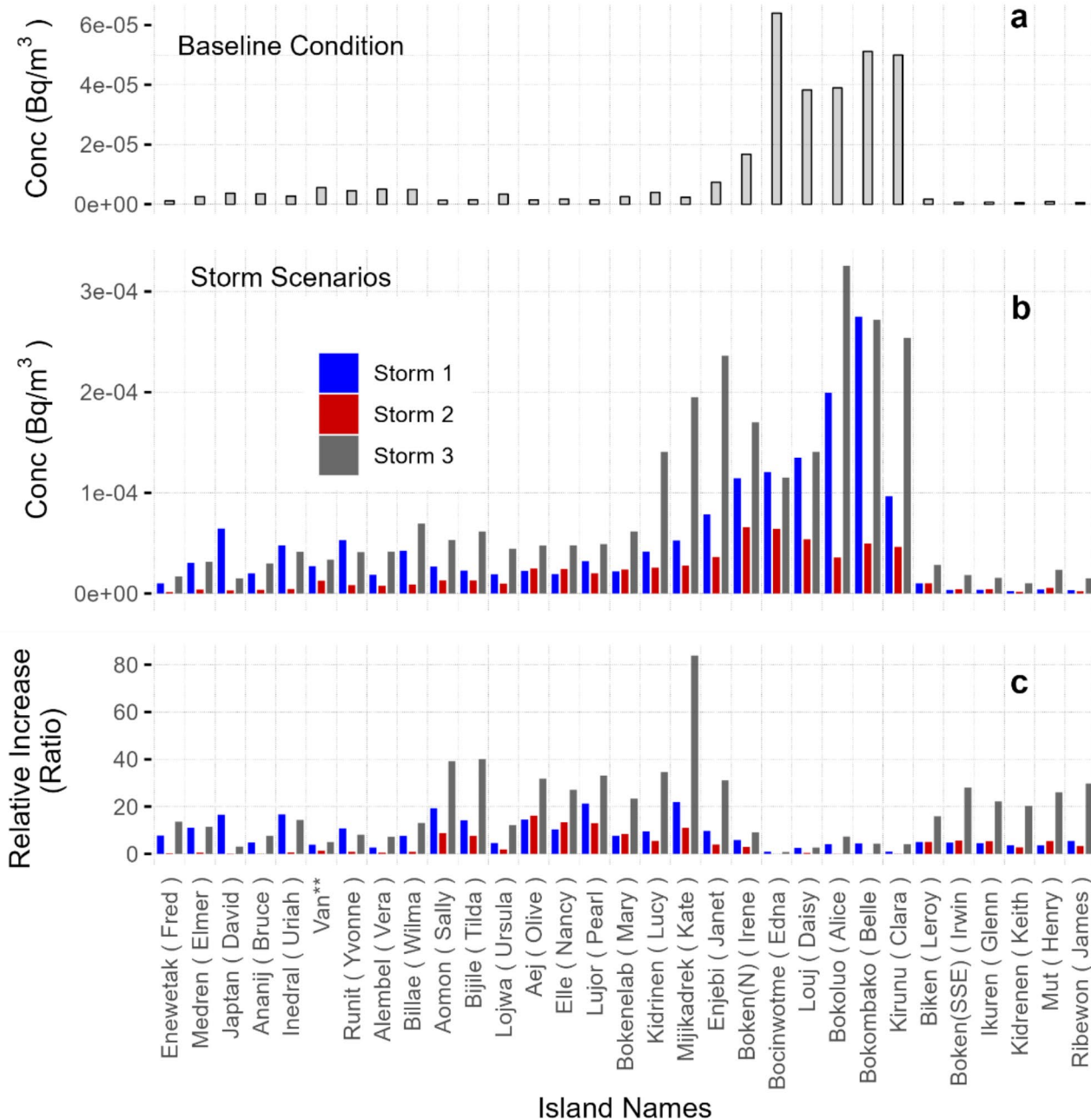
Current Climate (2015) Simulations of ^{239}Pu (Depth Average)

Fig. 17. The spatially (over depth and all receptor points around each island) and temporally (over 30-day period) averaged ^{239}Pu concentrations that each island is exposed to during the storm periods under current climate conditions. Note: These concentrations are incremental concentrations in addition to the existing background concentrations.

estimation of radionuclide inventory for the current year is entirely based on decades-old historical surveys, and biases/errors associated with historical instrumentations and technologies have been embedded. Due to the unavailability of reliable data sets to specify the kinetic parameter values related to sediment and biological processes, the model was not calibrated to reproduce the current background activity concentration levels ($^{137}\text{Cs} \approx 2.4 \text{ Bq/m}^3$, $^{239}\text{Pu} \approx 0.9 \text{ Bq/m}^3$)¹ of the lagoon waters, and instead, the model predicted the incremental activity concentrations using decay-corrected activity inventories. The radioactive decay corrected activities alone may not necessarily reflect or reproduce the current year's radionuclide activity of the lagoon due to other decaying processes such as biodegradation and natural flushing by the ocean currents. In addition to data limitations, the missing physical processes during storm conditions that have not been considered in the modeling may also add uncertainties to the results of the study. For instance, we did not consider the effect of storm-induced waves (i.e.,

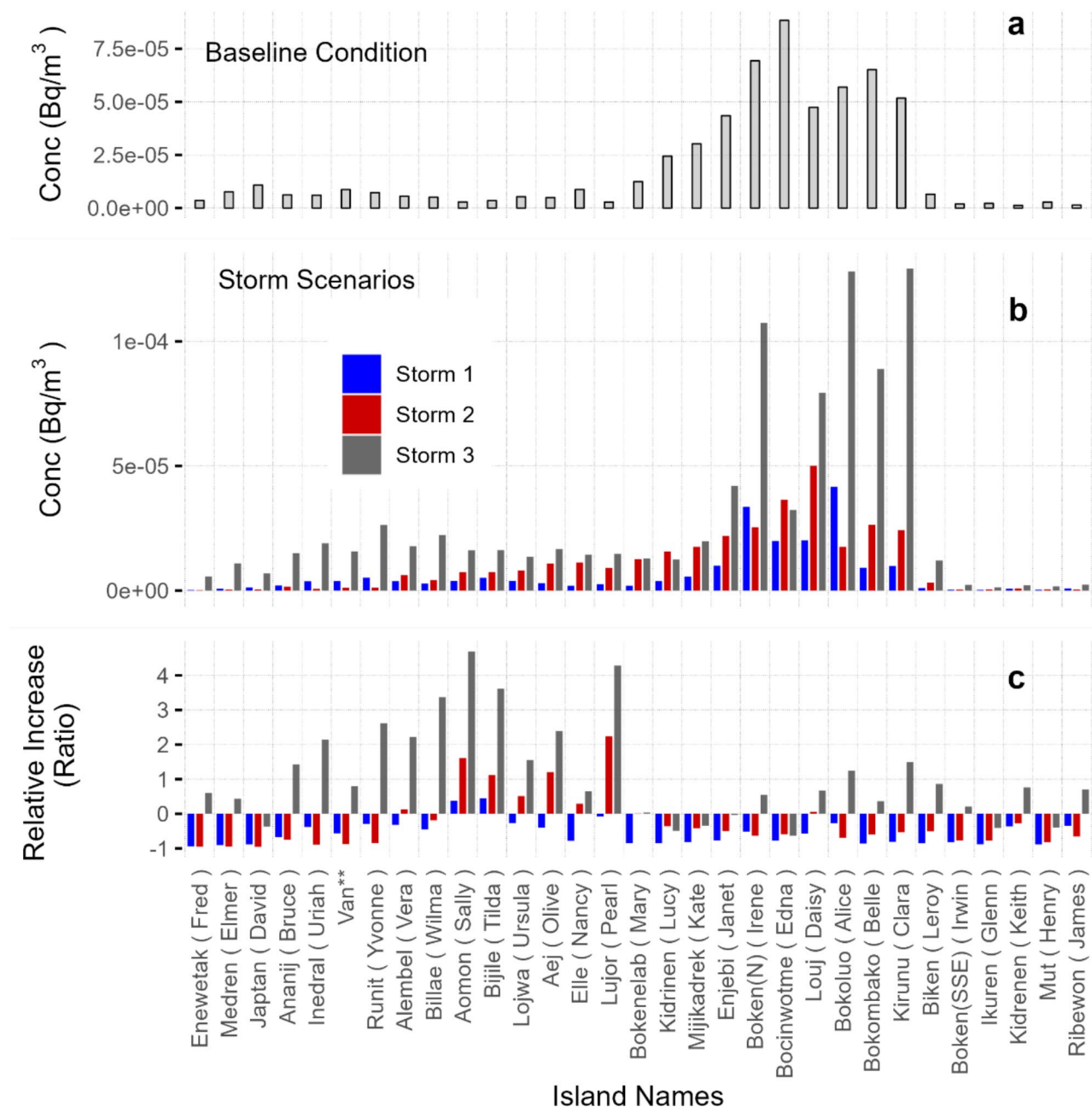
Future Climate (2090) Simulations of ^{239}Pu (Depth Average)

Fig. 18. The spatially (over depth and all receptor points around each island) and temporally (over 30-day period) averaged ^{239}Pu concentrations that each island is exposed to during the storm periods under future climate conditions. Note: These concentrations are incremental concentrations in addition to the existing background concentrations.

storm surge) in hydrodynamic modeling as it requires a detailed level of sub-scale parameterization for shallow water wave dynamics, which should be validated with site-specific data that is not available. However, the waves in shallow water areas may play an important role in the erosion process⁹. Although the fate and transport modeling has not considered the marine biological process and the immediate exposure radionuclide activities are significantly low concentrations, the perturbations from the storm may sustain a much longer time scale, and their impact on marine biota and terrestrial groundwater are important areas to be considered in future studies.

Summary and conclusion

We developed a numerical modeling framework to investigate the impact of extreme weather events, such as storms under current and future climates, on the radiologically contaminated Enewetak Atoll located in the

Future Climate (2090) Simulations of ^{239}Pu (Depth Average)

During a Hypothetical Dome Collapse Scenario

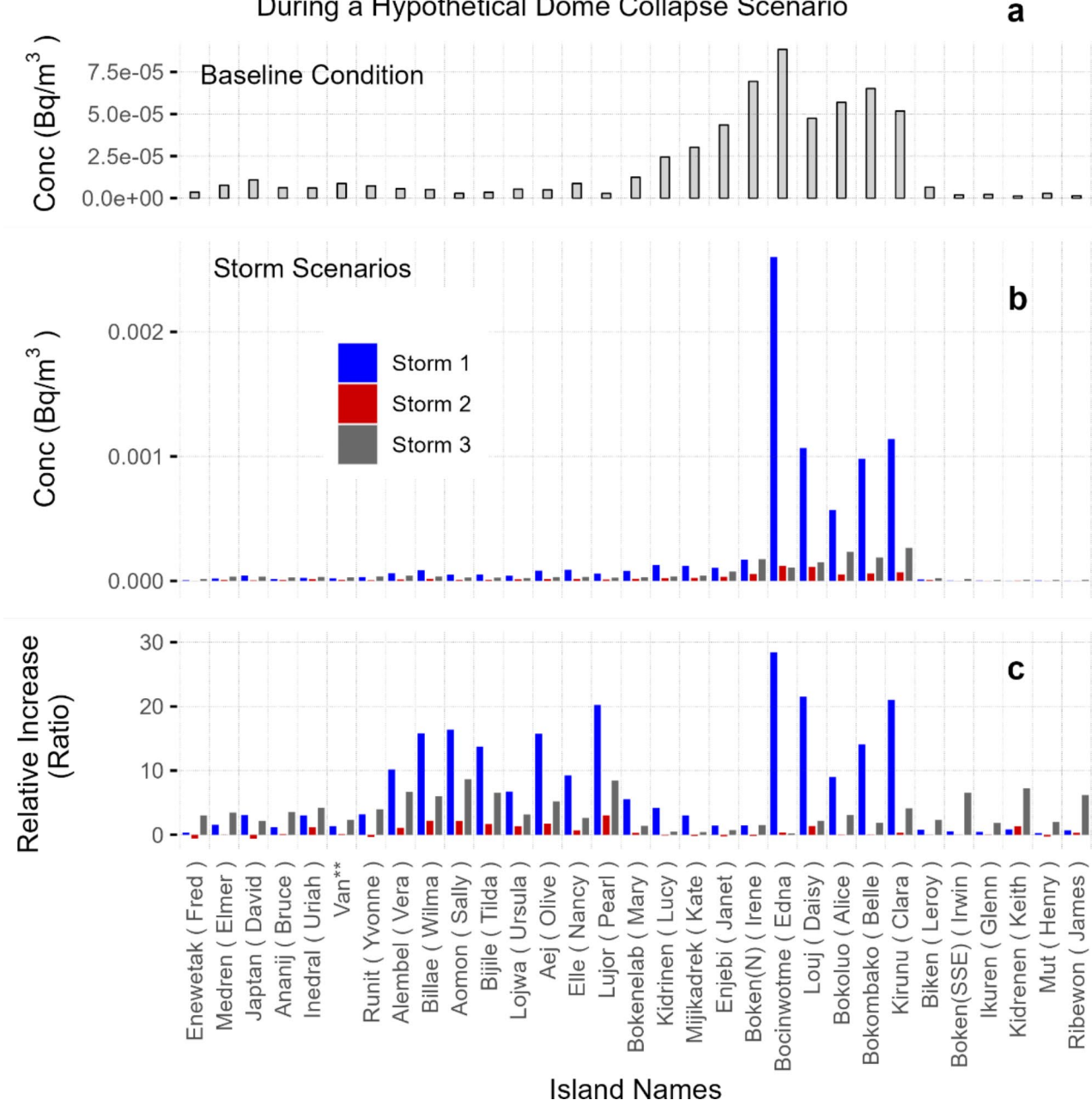


Fig. 19. The spatially (over depth and all receptor points around each island) and temporally (over 30-day period) averaged ^{239}Pu concentrations that each island is exposed to during the storm periods with hypothetical dome collapse under future climate conditions. These concentrations are incremental concentrations in addition to the existing background concentrations.

Republic of Marshall Islands. The objective of the study was to examine the potentially elevated radionuclide concentration due to storm-induced environmental conditions that may pose immediate exposure risks. The integrated modeling assessment was conducted by externally coupling three established models. WRF-ARW was used to reconstruct three selected storm scenarios that have the potential to impact the Atoll under current year (2015) and future year (2090) climates. Storm-induced meteorological conditions were then used to generate ocean hydrodynamics conditions using FVCOM. FVCOM-ICM was externally coupled with FVCOM-based hydrodynamics to simulate the fate and transport of radionuclides under sedimentation processes. A baseline scenario was established under the current year climate as well as settling and erosion processes, which are also in a dynamic steady state, to reflect the activity levels under regular environmental conditions without storms. The model simulations for radionuclide fate and transport under storm conditions were conducted for both

current (2015) and future (2090) climates. The elevated radionuclide concentrations predicted by the model were analyzed by comparing to the baseline activity concentration.

As shown by the model results, Storm 3 was the strongest storm that could inflict the highest impact on the Atoll and remobilized the sediments to increase the baseline concentration by several factors under both current and future climates. The maximum incremental ^{239}Pu concentration can reach up to 7.6 Bq/m^3 (in addition to existing background concentration¹ of 0.9 Bq/m^3) during the 30-day storm simulation period due to Storm 3, while the 30-day averaged maximum ^{239}Pu concentration that an island can be exposed to is $3.25\text{E-}4 \text{ Bq/m}^3$ under current climate conditions. The maximum relative increase that occurred under storm-induced wind shear at Island Mijikadrek (Kate) is 84 folds during Storm 3 period, while the mean relative increase for the Atoll is 20 folds under Storm 3 and the current climate. Despite the weakening of storms near the Atoll under future climate, a maximum ^{239}Pu concentration predicted during the storm period is 6.7 Bq/m^3 . However, the 30-day average maximum ^{239}Pu concentration is $1.3\text{E-}4 \text{ Bq/m}^3$, and a maximum relative increase of 4.7 was predicted for Island Aomon (Sally) for Storm 3 under future climate, which is a significant reduction compared to the relative increase under current climate conditions. However, the model scenario with a postulated collapse of Runit Dome under future climate conditions predicted a maximum relative increase of 28.4, indicating a potential risk of released contaminated sediments buried in Runit Dome. The peaks were noted during Storm 1 at Island Bocinwotme (Edna) and other northwestern islands, while the 30-day averaged maximum ^{239}Pu concentration was $2.6\text{E-}3 \text{ Bq/m}^3$. Overall, there is a potential to increase the existing/baseline radionuclide concentration of the Atoll on average by a factor of 20 due to the conditions induced by the strongest historical storm (Storm 3) under the current climate with close proximity to the Atoll simulated in the study. In contrast, under the future climate, Storm 3 caused a mean relative increase of only 1.1 for the Atoll, while Storm 1 caused a mean relative increase of 7.6 during a potential collapse of Runit Dome. It should be noted that despite the concentration increase due to the remobilization of radionuclide-bound sediments, the risk to human health and biota has to be evaluated with a comprehensive exposure assessment^{5,30}. We also note that the uncertainties/biases associated with the historical data and limitations of the modeling approach may have affected the results of this study and should be considered in further scientific investigations on the fate of the legacy contamination of Enewetak Atoll.

Data availability

"The model results produced in this study will be available in data hub of Pacific Northwest National Laboratory <https://data.pnnl.gov/>."

Received: 25 September 2024; Accepted: 6 January 2025

Published online: 15 January 2025

References

1. Buesseler, K. O., Charette, M. A., Pike, S. M. & Henderson, P. B. Kipp, L. E. Lingering radioactivity at the Bikini and Enewetak Atolls. *Sci. Total Environ.* **621**, 1185–1198 (2018).
2. AEC (United States Atomic Energy Commission). Enewetak Radiological Survey. NVO-140, **I** (1973).
3. DOE (United States Department of Energy). United States nuclear tests – July 1945 through September 1992. (2015).
4. Robison, W. L. & Noshkin, V. E. Radionuclide characterization and associated dose from long-lived radionuclides in close-in fallout delivered to the marine environment at Bikini and Enewetak Atolls. *Sci. Total Environ.* **237–238**, 311–327 (1999).
5. Prasad, R. et al. *Impacts of Climate Change on Human Health and the Environment in the Enewetak Atoll - PNNL-34408*. https://www.energy.gov/sites/default/files/2024-08/Report%20Appendix%20PNNL%20Climate%20Change%20Study-508_0.pdf (2024).
6. QGIS.org. QGIS Geographic Information System. Open Source Geospatial Foundation Project, version 3.22. <https://www.qgis.org/> (2021).
7. Noshkin, V. E. *Transuranium Radionuclides in Components of the Benthic Environment of Enewetak Atoll*. In *Transuranic Elements in the Environment*, Edited by Hanson, W.C. Prepared for U.S. Department of Energy. (1980).
8. Gwynn, J. P., Hatje, V., Casacuberta, N., Sarin, M. & Osvath, I. The effect of climate change on sources of radionuclides to the marine environment. *Commun. Earth Environ.* **5**, 135 (2024).
9. Xie, X., Li, M. & Ni, W. Roles of wind-driven currents and surface waves in sediment resuspension and transport during a tropical storm. *J. Geophys. Res. Oceans* **123**, 8638–8654 (2018).
10. Mooney, P. A., Mulligan, F. J., Bruyère, C. L., Parker, C. L. & Gill, D. O. Investigating the performance of coupled WRF-ROMS simulations of Hurricane Irene (2011) in a regional climate modeling framework. *Atmos. Res.* **215**, 57–74 (2019).
11. Kiran, P. V. & Balaji, C. The future projection of cyclones in Bay of Bengal: a study using coupled ocean atmosphere model. *Ocean. Dyn.* **72**, 641–660 (2022).
12. Mäll, M., Nakamura, R., Suursaar, Ü. & Shibayama, T. Pseudo-climate modelling study on projected changes in extreme extratropical cyclones, storm waves and surges under CMIP5 multi-model ensemble: Baltic Sea perspective. *Nat. Hazards* **102**, 67–99 (2020).
13. Green, M. O. & Coco, G. Review of wave-driven sediment resuspension and transport in estuaries: Wave-driven sediment transport. *Rev. Geophys.* **52**, 77–117 (2014).
14. Amoudry, L. O. & Souza, A. J. Deterministic coastal morphological and sediment transport modeling: a review and discussion. *Rev. Geophys.* **49**, 2010RG000341 (2011).
15. Warner, J. C., Armstrong, B., He, R. & Zambon, J. B. Development of a coupled ocean–atmosphere–wave–sediment transport (COAWST) modeling system. *Ocean. Model.* **35**, 230–244 (2010).
16. Jing, L. & Ridd, P. V. Modelling of suspended sediment transport in coastal areas under waves and currents. *Estuar. Coast Shelf Sci.* **45**, 1–16 (1997).
17. Liu, X. & Huang, W. Modeling sediment resuspension and transport induced by storm wind in Apalachicola Bay, USA. *Environ. Model. Softw.* **24**, 1302–1313 (2009).
18. Franz, G. et al. Modelling of sediment transport and morphological evolution under the combined action of waves and currents. *Ocean. Sci.* **13**, 673–690 (2017).
19. Periáñez, R. et al. Marine radionuclide transport modelling: recent developments, problems and challenges. *Environ. Model. Softw.* **122**, 104523 (2019).
20. Skamarock, W. C. et al. *A Description of the Advanced Research WRF Model Version 4.1*. <https://doi.org/10.5065/1dfh-6p97> (2019).
21. Atkinson, M., Smith, S. V. & Stroup, E. D. Circulation in Enewetak Atoll lagoon1. *Limnol. Oceanogr.* **26**, 1074–1083 (1981).

22. Monsen, N. E., Cloern, J. E., Lucas, L. V. & Monismith, S. G. A comment on the use of flushing time, residence time, and age as transport time scales. *Limnol. Oceanogr.* **47**, 1545–1553 (2002).
23. Noshkin, V. E. & Robison, W. L. Assessment of a radioactive waste disposal site at Enewetak Atoll. *Health Phys.* **73**, 234–247 (1997).
24. Simonoff, M., Sergeant, C., Poulain, S. & Pravikoff, M. S. Microorganisms and migration of radionuclides in environment. *Comptes Rendus Chim.* **10**, 1092–1107 (2007).
25. Chen, C., Liu, H. & Beardsley, R. C. An unstructured grid, finite-volume, three-dimensional, primitive equations ocean model: application to coastal ocean and estuaries. *J. Atmos. Ocean. Technol.* **20**, 159–186 (2003).
26. Kim, T. & Khangaonkar, T. An offline unstructured biogeochemical model (UBM) for complex estuarine and coastal environments. *Environ. Model. Softw.* **31**, 47–63 (2012).
27. Khangaonkar, T. et al. Analysis of hypoxia and sensitivity to nutrient pollution in Salish sea. *J. Geophys. Res. Oceans* **123**, 4735–4761 (2018).
28. Khangaonkar, T., Long, W. & Xu, W. Assessment of circulation and inter-basin transport in the salish sea including Johnstone strait and discovery islands pathways. *Ocean. Model.* **109**, 11–32 (2017).
29. Higashi, H., Morino, Y., Furuichi, N. & Ohara, T. Ocean dynamic processes causing spatially heterogeneous distribution of sedimentary caesium-137 massively released from the Fukushima Daiichi nuclear power plant. *Biogeosciences* **12**, 7107–7128 (2015).
30. Prasad, R. et al. Assessing effects of climate change on legacy waste at the enewetak atoll. In *WM2024 Conference* (Phoenix, Arizona, USA).

Acknowledgements

We appreciate and acknowledge the funding and background knowledge provided by the Department of Energy's Office of Environment, Health, Safety, and Security for the success of this work. Also, we acknowledge the staff at Lawrence Livermore National Laboratory, the U.S. Geological Survey, and independent researchers for sharing expertise and knowledge and the support and encouragement provided by the Pacific Northwest National Laboratory.

Author contributions

"L.P. prepared the original manuscript, analysis, fate, and transport simulations. S.G. supported the original manuscript, data analysis, and contaminant characterization. R.P. supervised the overall study and reviewed the manuscript. S.T. atmospheric modeling and storm simulations. T.W. ocean modeling. T.K. supervised the ocean modeling and fate and transport simulations. B.N. contaminant characterization and supervision. T.I. contaminant characterization and supervision. L.L. supervised the atmospheric modeling and storm simulations."

Declarations

Competing interests

The authors declare no competing interests.

Additional information

Supplementary Information The online version contains supplementary material available at <https://doi.org/10.1038/s41598-025-85849-8>.

Correspondence and requests for materials should be addressed to L.P.

Reprints and permissions information is available at www.nature.com/reprints.

Publisher's note Springer Nature remains neutral with regard to jurisdictional claims in published maps and institutional affiliations.

Open Access This article is licensed under a Creative Commons Attribution-NonCommercial-NoDerivatives 4.0 International License, which permits any non-commercial use, sharing, distribution and reproduction in any medium or format, as long as you give appropriate credit to the original author(s) and the source, provide a link to the Creative Commons licence, and indicate if you modified the licensed material. You do not have permission under this licence to share adapted material derived from this article or parts of it. The images or other third party material in this article are included in the article's Creative Commons licence, unless indicated otherwise in a credit line to the material. If material is not included in the article's Creative Commons licence and your intended use is not permitted by statutory regulation or exceeds the permitted use, you will need to obtain permission directly from the copyright holder. To view a copy of this licence, visit <http://creativecommons.org/licenses/by-nc-nd/4.0/>.

© Battelle Memorial Institute 2025